Received: 18 December 2019 | Revised: 30 April 2020 | Accepted: 1 May 2020

DOI: 10.1002/asl.984

RESEARCH ARTICLE

Atmospheric Science Letters RMetS

Twenty first century changes in Antarctic and Southern Ocean surface climate in CMIP6

Thomas J. Bracegirdle[1] | **Gerhard Krinner**[2] | **Marcos Tonelli**[3] | **F. Alexander Haumann**[4] | **Kaitlin A. Naughten**[1] | **Thomas Rackow**[5] | **Lettie A. Roach**[6] | **Ilana Wainer**[3]

[1]British Antarctic Survey, Cambridge, UK

[2]CNRS, Université Grenoble Alpes, Institut des Géosciences de l'Environnement (IGE), Grenoble, France

[3]Instituto Oceanográfico, Universidade de Sao Paulo, Sao Paulo, Brazil

[4]Atmospheric and Oceanic Sciences Program, Princeton University, Princeton, New Jersey

[5]Alfred Wegener Institute, Helmholtz Centre for Polar and Marine Research, Climate Dynamics, Bremerhaven, Germany

[6]Atmospheric Sciences, University of Washington, Seattle, Washington

Correspondence
Thomas J. Bracegirdle, British Antarctic Survey, Madingley Road, Cambridge, CB3 0ET, UK.
Email: tjbra@bas.ac.uk

Funding information
British Antarctic Survey, Grant/Award Numbers: NE/L013770/1, NE/N01829X/1; National Oceanic and Atmospheric Administration, Grant/Award Number: NA18OAR4310274; National Science Foundation, Grant/Award Numbers: PLR-1425989, PLR-1643431; Swiss National Science Foundation, Grant/Award Numbers: P2EZP2_175162, P400P2_186681

Abstract

Two decades into the 21st century there is growing evidence for global impacts of Antarctic and Southern Ocean climate change. Reliable estimates of how the Antarctic climate system would behave under a range of scenarios of future external climate forcing are thus a high priority. Output from new model simulations coordinated as part of the Coupled Model Intercomparison Project Phase 6 (CMIP6) provides an opportunity for a comprehensive analysis of the latest generation of state-of-the-art climate models following a wider range of experiment types and scenarios than previous CMIP phases. Here the main broad-scale 21st century Antarctic projections provided by the CMIP6 models are shown across four forcing scenarios: SSP1-2.6, SSP2-4.5, SSP3-7.0 and SSP5-8.5. End-of-century Antarctic surface-air temperature change across these scenarios (relative to 1995–2014) is 1.3, 2.5, 3.7 and 4.8°C. The corresponding proportional precipitation rate changes are 8, 16, 24 and 31%. In addition to these end-of-century changes, an assessment of scenario dependence of pathways of absolute and global-relative 21st century projections is conducted. Potential differences in regional response are of particular relevance to coastal Antarctica, where, for example, ecosystems and ice shelves are highly sensitive to the timing of crossing of key thresholds in both atmospheric and oceanic conditions. Overall, it is found that the projected changes over coastal Antarctica do not scale linearly with global forcing. We identify two factors that appear to contribute: (a) a stronger global-relative Southern Ocean warming in stabilisation (SSP2-4.5) and aggressive mitigation (SSP1-2.6) scenarios as the Southern Ocean continues to warm and (b) projected recovery of Southern Hemisphere stratospheric ozone and its effect on the mid-latitude westerlies. The major implication is that over coastal Antarctica, the surface warming by 2100 is stronger relative to the global mean surface warming for the low forcing compared to high forcing future scenarios.

KEYWORDS
Antarctic, climate, CMIP6, projection, Southern Ocean, westerlies

1 | INTRODUCTION

Changes in the Antarctic and Southern Ocean (SO) climate system are of global importance. The response of the Antarctic ice sheet in a warming world is a major component of projected 21st century changes in global sea level (DeConto and Pollard, 2016; Rohling *et al.*, 2019). The rate of anthropogenic heat and carbon uptake in the SO is a key influence on the rate of global warming not just in the future, but in the present day (Frölicher *et al.*, 2015; Hwang *et al.*, 2017; Bushinsky *et al.*, 2019; Gruber *et al.*, 2019). Within the region, sensitive ecosystems are projected to be strongly affected by, for example, changes in sea ice extent, ice-free land area and regional warming (Jenouvrier *et al.*, 2014; Turner *et al.*, 2014; Lee *et al.*, 2017; Rintoul *et al.*, 2018). Therefore, although isolated geographically from the main concentrations of human population, Antarctica is at the centre of one of the major regulators and drivers of climate change globally. The question of how Antarctic climate will change under scenarios of future anthropogenic forcing is therefore key in the evaluation of climate model projections of 21st century climate.

Climate and Earth System Models (ESMs) (referred to collectively as climate models hereinafter) are the main tools used for quantitatively estimating how 21st century climate may evolve under different scenarios of future anthropogenic activity. Progress in improving Antarctic climate projections until the end of this century has been greatly helped in recent years by the vast archive of climate model output from major modelling centres coordinated by the World Climate Research Programme's Coupled Model Intercomparison Project Phase 5 (CMIP5) (Taylor *et al.*, 2012). However, the CMIP5 models are, at time of writing, approximately a decade old and many improvements and advances have now been implemented by climate model centres. Widespread large biases in sea ice extent and mid-latitude westerlies affect the accuracy of future projections made by those models (Bracegirdle *et al.*, 2015). The sixth CMIP (CMIP6) (Eyring *et al.*, 2016) is now providing an updated source of data for estimating 21st century climate change. In addition to model development, a key advance since CMIP5 is an updated range of future forcing scenarios, compiled as a specific endorsed CMIP6 project, ScenarioMIP (O'Neill *et al.*, 2016). The scenarios are developed around different Shared Socioeconomic Pathways (SSPs), but also include radiative forcing targets for 2100 as seen in the previous Representative Concentration Pathways (RCPs) (Meinshausen *et al.*, 2011). The tier 1 SSP's are SSP1-2.6, SSP2-4.5, SSP3-7.0 and SSP5-8.5, which nominally span the same radiative forcing range as RCP2.6 to RCP8.5.

When evaluating Antarctic projections based on CMIP6, it is important to consider that potentially important improvements remain a priority for current and future model development. In the Antarctic region, the atmosphere is tightly coupled to other components of the Earth system, such as the ocean and the cryosphere. Changes in these components affect the climate both locally and globally. For example, increased meltwater flux from the Antarctic Ice Sheet into the SO is expected to counteract some of the surface atmospheric warming caused by climate change (Hansen *et al.*, 2016; Bronselaer *et al.*, 2018; Golledge *et al.*, 2019). This meltwater is expected to impact the ocean's overturning circulation and also affect precipitation patterns and temperature variability worldwide. Melting and retreat of the Antarctic Ice Sheet, and the subsequent impacts on climate, are not represented in standard-configuration CMIP6 models. Additionally, insufficient resolution also means that important SO and ice sheet marginal processes are still missing. For example, mesoscale eddies are a major source of ocean heat transport onto the Antarctic continental shelf (Stewart and Thompson, 2015; Goddard *et al.*, 2017; Thompson *et al.*, 2018). Currently, the first coupled ice sheet-ocean models are becoming operational (Asay-Davis *et al.*, 2016; De Rydt and Gudmundsson, 2016; Hellmer *et al.*, 2017; Favier *et al.*, 2019), and the SO modelling community is aiming to incorporate these advances into CMIP7 configurations.

Given the importance of Antarctic coastal processes, we will look not only at Antarctic mean quantities, but also at latitudinal cross sections across coastal Antarctica and the SO. Of particular interest is scenario dependence of trajectories of 21st century change and the potential of more rapid Antarctic warming relative to the rest of the globe in stabilisation and mitigation scenarios. Model simulations and paleo reconstructions show this more pronounced global-relative Antarctic warming (hereinafter "global-relative" refers to the ratio of change in a given region to global mean change) emerging on long timescales as the damping effect of SO heat uptake recedes (Manabe *et al.*, 1991; Li *et al.*, 2013; Armour *et al.*, 2016). Delayed warming responses of the SO in models and observations have been attributed to the background (mean) ocean overturning (Armour *et al.*, 2016) and can continue to occur over multiple centuries in stabilisation

scenarios. In the aggressive mitigation scenario SSP1-2.6, global mean surface air temperature (GSAT) stabilizes mid-century and in fact cools slightly by 2100 (O'Neill *et al*., 2016), during which the SO may exhibit a continued delayed warming. A key question is, therefore, the extent to which this delaying effect may contribute to continued warming at high southern latitudes even in aggressive mitigation and stabilisation scenarios. In evaluating contrasts between high and low forcing scenarios, it is recognized that the standard CMIP6 model configurations assessed here do not include impacts of freshwater input from melting ice shelves (Bronselaer *et al*., 2018), which is a potentially important mechanism for preferentially stronger delays/damping in SO warming in high emissions scenarios. The implications of this are revisited in the Conclusions section. This is of particular relevance to coastal Antarctica, where, for example, ecosystems and ice shelves are highly sensitive to the timing of crossing of key thresholds in both atmospheric and oceanic conditions (Golledge *et al*., 2017; Hellmer *et al*., 2017).

In addition to the potential for the emergence of delayed SO global-relative warming in stabilisation scenarios, recovery of stratospheric ozone (Eyring *et al*., 2007; Wilcox *et al*., 2012) is a key consideration as a driver of trends that contrast with the mean global forcing (Perlwitz *et al*., 2008; Son *et al*., 2008; Karpechko *et al*., 2010; Smith *et al*., 2012). In particular, in CMIP5 it was found that in the first half of the 21st century stratospheric ozone recovery acts to shift the westerly jet equatorward, but that this is cancelled out by GHG increases acting in the opposite direction and resulting in no significant change (Barnes *et al*., 2014). During the second half of the 21st century the ozone forcing weakens and the westerly jet shifts southward more strongly. In the four SSP scenarios considered here it can likely be assumed that similar rates of stratospheric ozone recovery occur across the range of scenarios as identified for the equivalent RCP scenarios by Dhomse *et al*. (2018).

In this paper, the above factors will be considered in quantifying 21st century climate change over Antarctica and the SO. A comprehensive assessment of cause and effect is outside the scope of this initial assessment of the new CMIP6 dataset. The aim instead is to quantify the broad-scale projections from present-day to 2100 with a view to more detailed evaluations in the future. Specific questions addressed here are:

- What are the projected 21st century changes in Antarctic surface temperature, precipitation rate and the westerly winds as simulated across the four tier-1 SSPs of CMIP6?
- Does the delayed response of the SO lead to the emergence of a significantly stronger global-relative Antarctic and SO warming in the strong mitigation and stabilisation SSPs (SSP1-2.6 and SSP2-4.5)?

2 | DATA AND METHODS

2.1 | CMIP6 data

The main source of data is the CMIP6 archive. At time of writing data from 15 models were available for the range of scenarios and variables used, which are outlined in Table 1. Baseline time-mean climatologies were calculated from the 1995–2014 time slice of output from historical CMIP6 runs. The four tier-one ScenarioMIP future forcing experiments, SSP1-2.6, SSP2-4.5, SSP3-7.0 and SSP5-8.5, were used for assessing 21st century projections. For each run, monthly mean output was extracted for the following variables: surface air temperature at 2 m (SAT) (CMIP6 variable name "tas"), sea surface temperature (SST) ("tos"), zonal wind at 850 hPa (UA850) ("ua") and surface precipitation rate (PR) ("pr"). For each of models the first realisation was used.

2.2 | Spatial mean diagnostics

2.2.1 | Antarctic continent

The outline and topography of the Antarctic continent in CMIP6 models was determined from the native masks ("sftlf") and orography ("orog") when available. When these were unavailable, we interpolated the corresponding fields from CNRM-CM6-1 onto the respective model grid. Area-weighted spatial means were then calculated across all land

TABLE 1 List of CMIP6 models used in this study. Expansions of institution acronyms are available at https://wcrp-cmip.github.io/CMIP6_CVs/docs/CMIP6_institution_id.html

Model number	Model centre	Model name
1	AWI	AWI-CM-1-1-MR
2	BCC	BCC-CSM2-MR
3	CAMS	CAMS-CSM1-0
4	CCCma	CanESM5
5	CNRM-CERFACS	CNRM-CM6-1
6	CNRM-CERFACS	CNRM-ESM2-1
7	CSIRO	ACCESS-ESM1-5
8	CSIRO-ARCCSS	ACCESS-CM2
9	IPSL	IPSL-CM6A-LR
10	MIROC	MIROC6
11	MOHC	UKESM1-0-LL
12	MPI-M DWD DKRZ	MPI-ESM1-2-HR
13	MRI	MRI-ESM2-0
14	NCAR	CESM2
15	NCAR	CESM2-WACCM

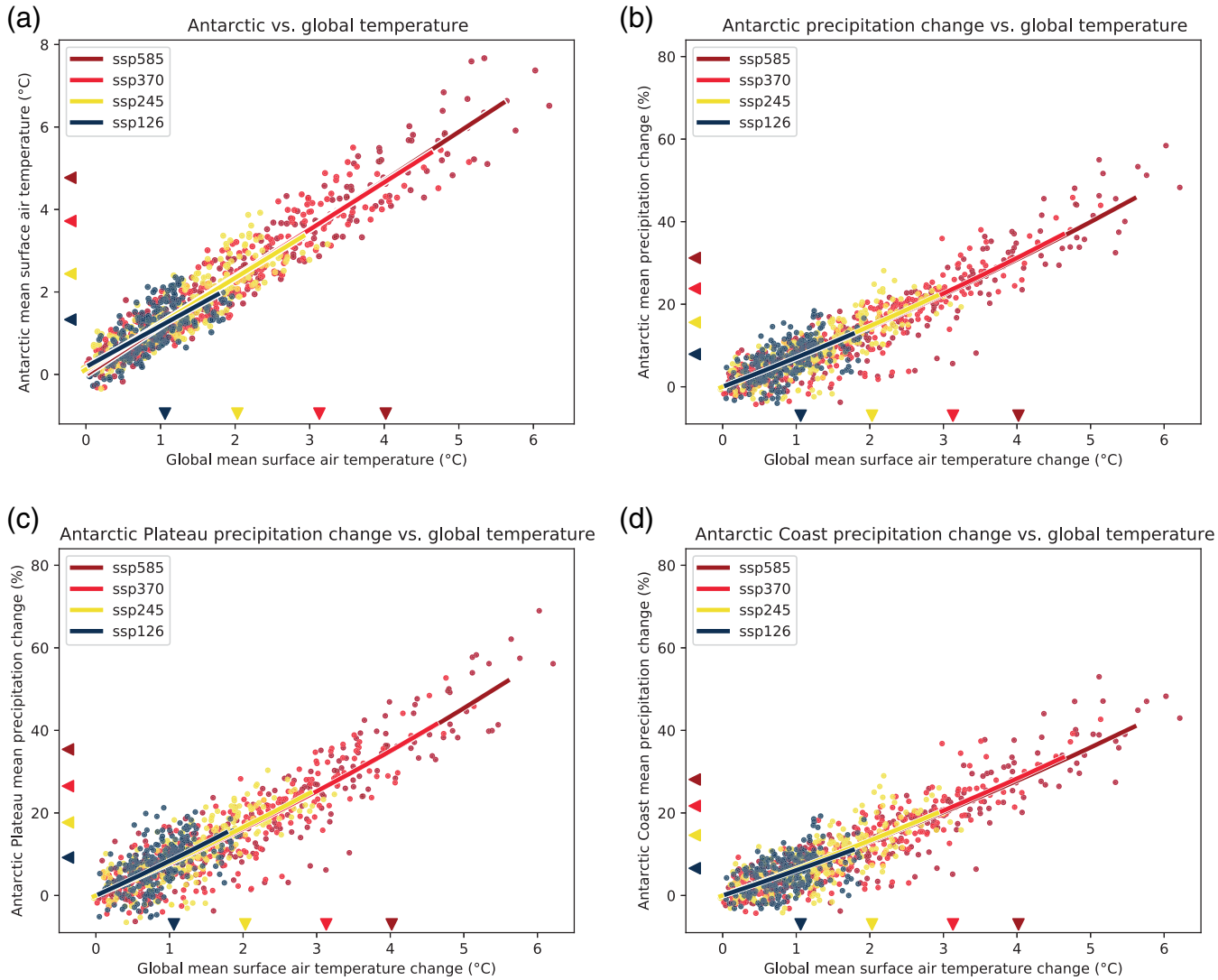

FIGURE 1 (a) Antarctic versus global mean SAT change for all available models (1st ensemble member) and four scenarios. Each dot is a 5-year average time-slice difference relative to the 1995–2014 mean. Regression lines are shown to quantify possible inter-scenario differences in GSAT-relative temperature projections. (b–d) Antarctic precipitation change against GSAT change (b), and separately also over the plateau (h > 1,500) (c) and at coastal regions (h < 1,500 m) (d). The regression lines in (b–d) are an exponential fit y = exp(a*T) − 1

and ice sheet regions of Antarctica, including floating ice shelves. For the diagnoses of precipitation and temperature changes over the Antarctic continent, 5-year averages were taken relative to the 1995–2014 mean. Similarly, area-weighted GSAT changes were calculated as 5-year averages relative to 1995–2014.

2.2.2 | Southern Ocean

The sea surface temperature (SST) outputs from each model were firstly interpolated onto the same regular 360 × 180 grid for consistency. The global mean was computed by integrating the area-weighted SST average for each time slice considered. The Southern Hemisphere (SH) SST was computed as the zonal mean from the Equator to 80°S. Similar to SAT, the relative change was computed as zonally averaged SST difference (2080–2100 minus 1995–2014) for the SH divided by the global area-weighted SST (GSST) difference for the same period.

The SO time series were computed as annual means of the area-weighted SST between 60 and 80°S. The first-year annual mean (2015) is subtracted from each time series yielding the actual SST change over each SSP scenario projection.

2.3 | Westerly jet indices

The westerly jet latitude index (JLI) is defined as the latitude of the maximum in zonally-averaged tropospheric

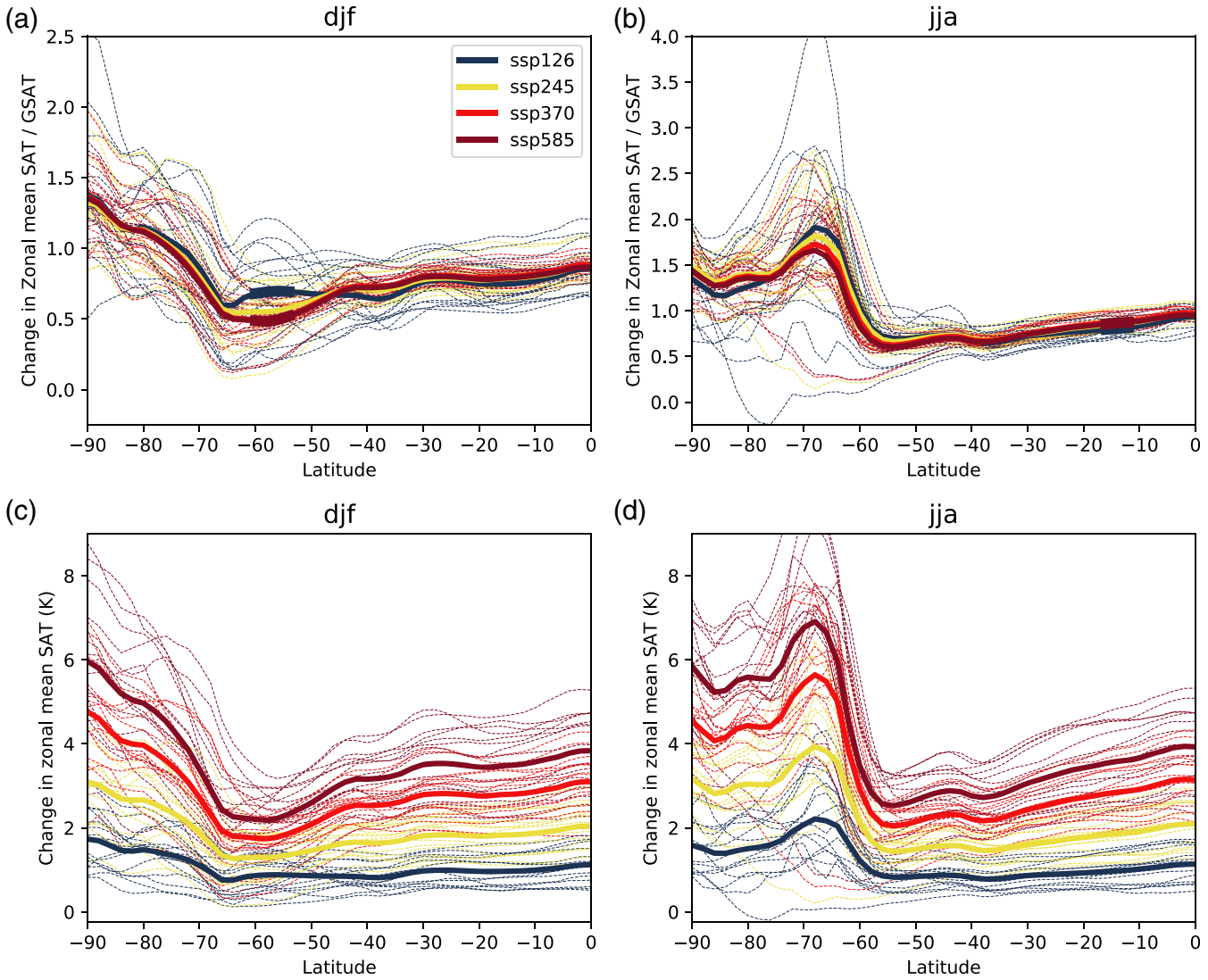

FIGURE 2 Twenty first century zonal mean SAT change in summer (December–February) (a, c) and winter (June–August) (b, d) presented both relative to GSAT change (a, b) and as absolute change (c, d). Changes are defined as differences between time slice means over 2081–2100 in future scenario simulations and 1995–2014 in historical simulations. Thin dotted lines indicate individual ensemble members and solid lines indicate ensemble means for each scenario. In (a) and (b) thicker sections of solid lines for SSP1-2.6 and SSP5-8.5 ensemble means denote latitudes at which inter-scenario differences are significant at the $p = .05$ level (based on a t test of the difference between the n model values in each of these two scenarios, where the ensemble size n is 15 in this case)

zonal wind on the 850 hPa pressure level (UA850). For each monthly mean field of interest, the maximum in zonal mean UA850 between latitudes of 75°S and 10°S defines the jet speed, the latitude of which defines the jet latitude. The annual and seasonal jet latitude index and jet speed index (JSI) were constructed from averages of jet latitudes calculated for each month of the year or season of interest.

3 | RESULTS

In the first part of this section we present an overview of full-century changes. This is followed by a more detailed assessment of change in the first and second halves of 21st century, motivated by the larger inter-scenario divergence in the later period and the impacts of stratospheric ozone recovery across these scenarios.

3.1 | 21st century projections

Over the 21st century, SAT over the Antarctic continent is projected to increase across a wide range of scenarios (Figure 1a). CMIP6 multi-model mean end-of-century annual-mean warming relative to 1995–2014 is 1.3 ± 0.5, 2.5 ± 0.7, 3.7 ± 0.9 and 4.8 ± 1.2°C (the ranges shown

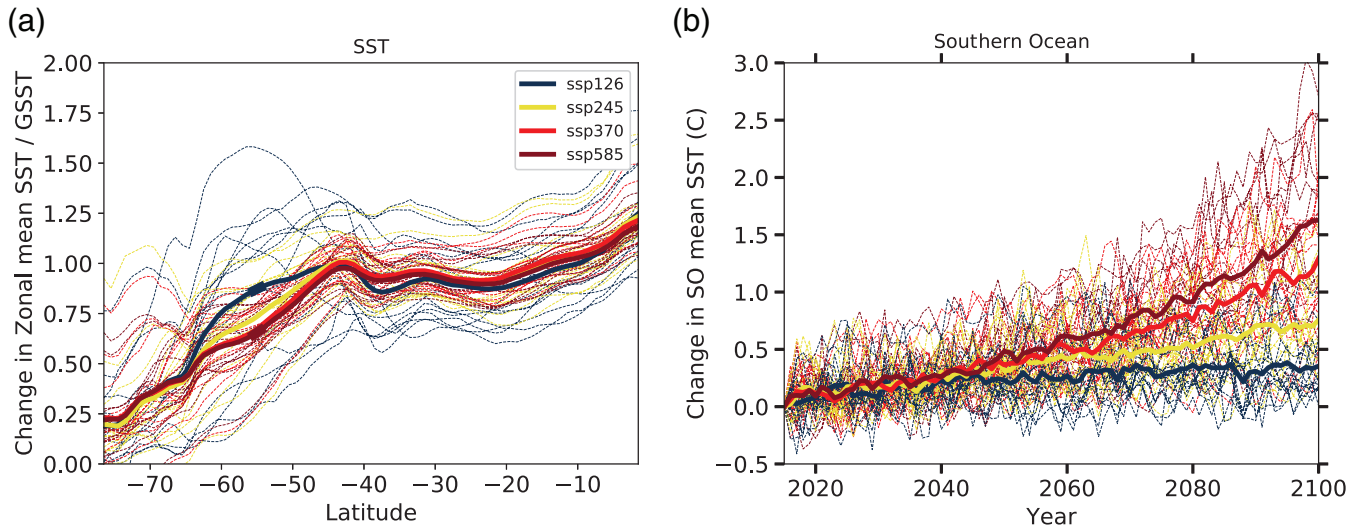

FIGURE 3 (a) 21st-century zonal mean SST change relative to GSST change. As in Figure 2, changes are defined as differences between time slice means over 2081–2100 and 1995–2014. (b) Absolute SST change (annual means) in the Southern Ocean relative to 2015 for future scenarios. Lines are defined as is Figure 2 and as in Figure 2a,b, thicker sections of the solid lines in (a) show latitudes of statistically significant inter-scenario differences between SSP1-2.6 and SSP5-8.5

are standard deviations of the model values) following the SSP1-2.6, SSP2-4.5, SSP3-7.0 and SSP5-8.5 scenarios respectively. Unlike in the Arctic, there is no clear polar amplification over the continent (Salzmann, 2017), with Antarctic warming only marginally stronger than global mean GSAT warming (Figure 1a). Given the proximity of the SO and potential scenario dependence of its delayed response, it is perhaps surprising that the relationship between global and Antarctic continental warming remains almost identical in different decades and scenarios through the 21st century. In addition to the potential effects of delayed SO warming response, stratospheric ozone recovery provides a regional forcing that can induce trends deviating from the global mean (Barnes *et al*., 2014).

To investigate these points in more detail, Figure 2 shows the latitudinal and seasonal dependence of 21st century SAT change across the same range of scenarios. Both absolute and GSAT-relative changes are shown. Over the SO and into coastal Antarctica stronger GSAT-relative increases are evident in SSP1-2.6 and SSP2-4.5 compared to higher forcing scenarios, particularly in the latitude range of approximately 50°S to 65°S in summer (DJF) (for which differences between SSP1-2.6 and SSP5-8.5 are statistically significant at $p < .05$ level) and extending to a higher-latitude maximum between 65°S and 70°S in winter (JJA). This higher latitude range extends over much of coastal East Antarctica and the sub-polar seas around West Antarctica. In these regions enhanced near-surface warming in JJA is associated with low altitude warming as sea ice retreats and exposes the atmosphere to increased heat fluxes from the ocean (Bromwich *et al*., 1998; England *et al*., 2018). This seasonal and regional effect is however too weak to emerge in the annual-mean continental-mean changes shown in Figure 1a. A key implication is therefore that scenario-dependent GSAT-relative warming is most prominent along coastal Antarctica and changes here do not scale with global mean change in a simple way. Note that the inter-scenario differences over coastal Antarctica in winter between SSP1-2.6 and SSP5-8.5 are not statistically significant (Figure 2b). This may be due to large inter-model differences in sea ice retreat making it more difficult to distinguish inter-scenario differences associated with SST. However, a similar analysis of annual mean SSTs shown in Figure 3a gives qualitatively similar inter-scenario differences with relatively strong warming in the weaker forcing scenarios, in particular the SSP1-2.6 to SSP5-8.5 differences are statistically significant equatorward of coastal East Antarctica at about 65°S. The higher latitude maximum in winter SAT (and associated inter-scenario differences) (Figure 2b) is likely to be mainly a consequence of a larger impact near-surface warming associated with retreat of sea ice.

The weaker global-relative SO warming in high-forcing scenarios SSP3-7.0 and SSP5-8.5 is consistent with more rapid heat uptake associated with rapid and sustained forcing and transient warming through the year 2100 in these scenarios (O'Neill *et al*., 2016). In SSP2-4.5 total anthropogenic radiative forcing has stabilized by 2100 and is, along with GSAT, declining in SSP1-2.6 (O'Neill *et al*., 2016). Figure 3b shows however that the SO does not yet show

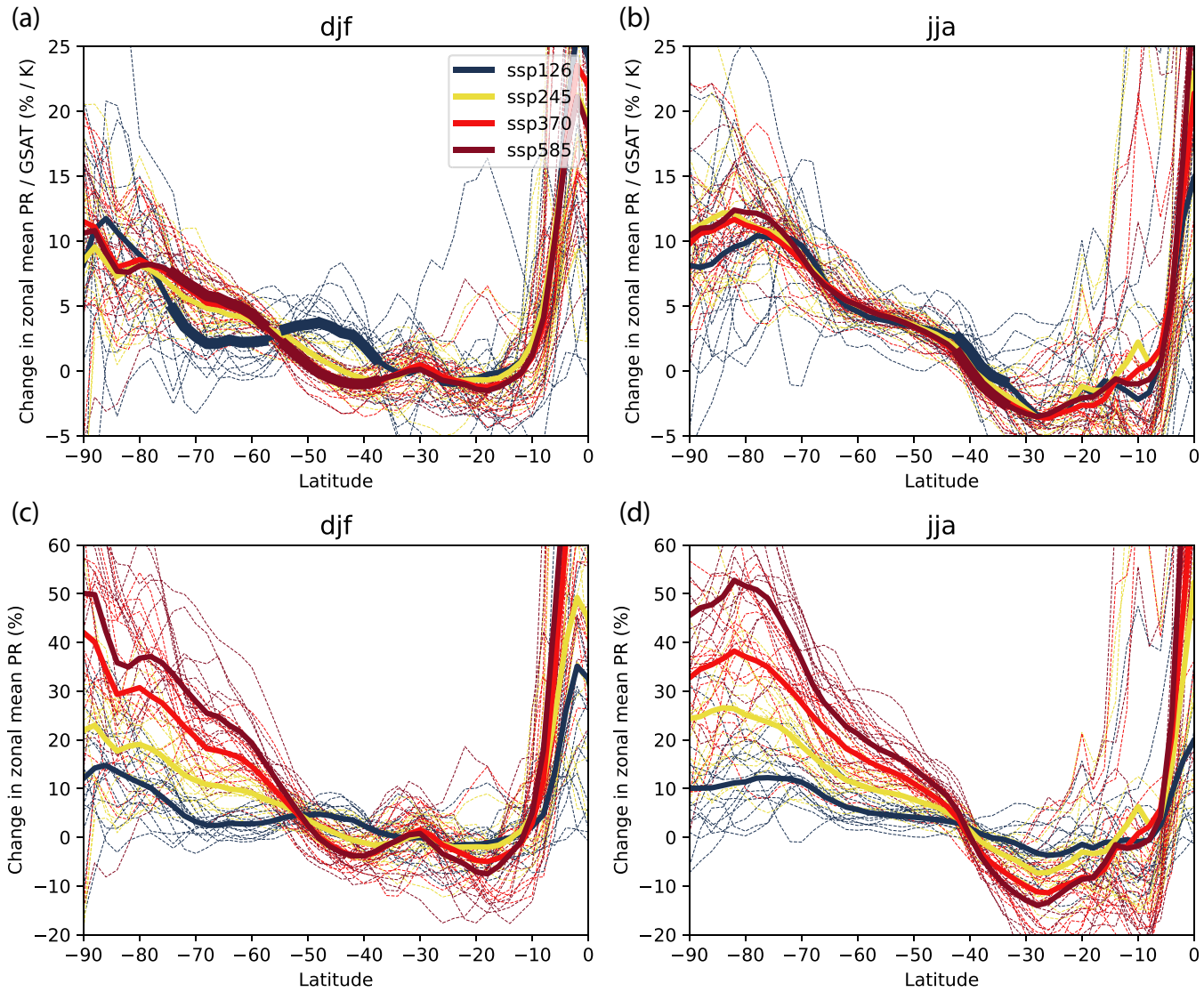

FIGURE 4 As in Figure 2, but for precipitation rate (i.e., the upper row (a, b) shows change relative to global mean warming in $m \cdot s^{-1} \cdot K^{-1}$)

evidence of a late-century onset of decreases in sea-surface temperature in any scenario.

For PR, multi-model mean 21st century annual mean increases following the SSP1-2.6, SSP2-4.5, SSP3-7.0 and SSP5-8.5 scenarios are 8 ± 5, 16 ± 6, 24 ± 9 and 31 ± 12%, respectively (Figure 1b). There is a suggestion of weakly contrasting pathways for Antarctic-wide annual-mean change relative to GSAT (Figure 1b–d). In all scenarios it was found that an exponential model provides slightly better fits than a linear model (RMSE on average 5% smaller for the SSP3-7.0 and SSP5-8.5 scenarios), which is consistent with the fact that the saturation vapour pressure air increases nonlinearly with temperature according to the Clausius Clapeyron relation.

Over the SO, scenario-dependence of GSAT-relative PR change is much weaker at mid-to-high southern latitudes in winter (JJA) compared to summer (DJF) (Figure 4), when surface circulation responses to stratospheric ozone change are strongest (Thompson and Solomon, 2002). The summer changes are most strikingly different in the SSP1-2.6 scenario, with decreases towards coastal Antarctica and increases at mid-latitudes, equatorward of the climatological westerly jet core at ~50°S. This is consistent with an overall equatorward shift of the tropospheric eddy-driven jet (and associated storm track) in the low radiative forcing scenario SSP1-2.6 (Figure 5). Climate impacts of stratospheric ozone recovery will be of greater relative importance in the latter half of the 21st century, when the greenhouse gas forcing has stabilised and is in fact decreasing slightly (O'Neill *et al.*, 2016). While it is true that the main period of stratospheric ozone recovery is projected to occur in the first half of the 21st century, the results here suggest that under the SSP1-2.6 scenario the continued less rapid ozone recovery

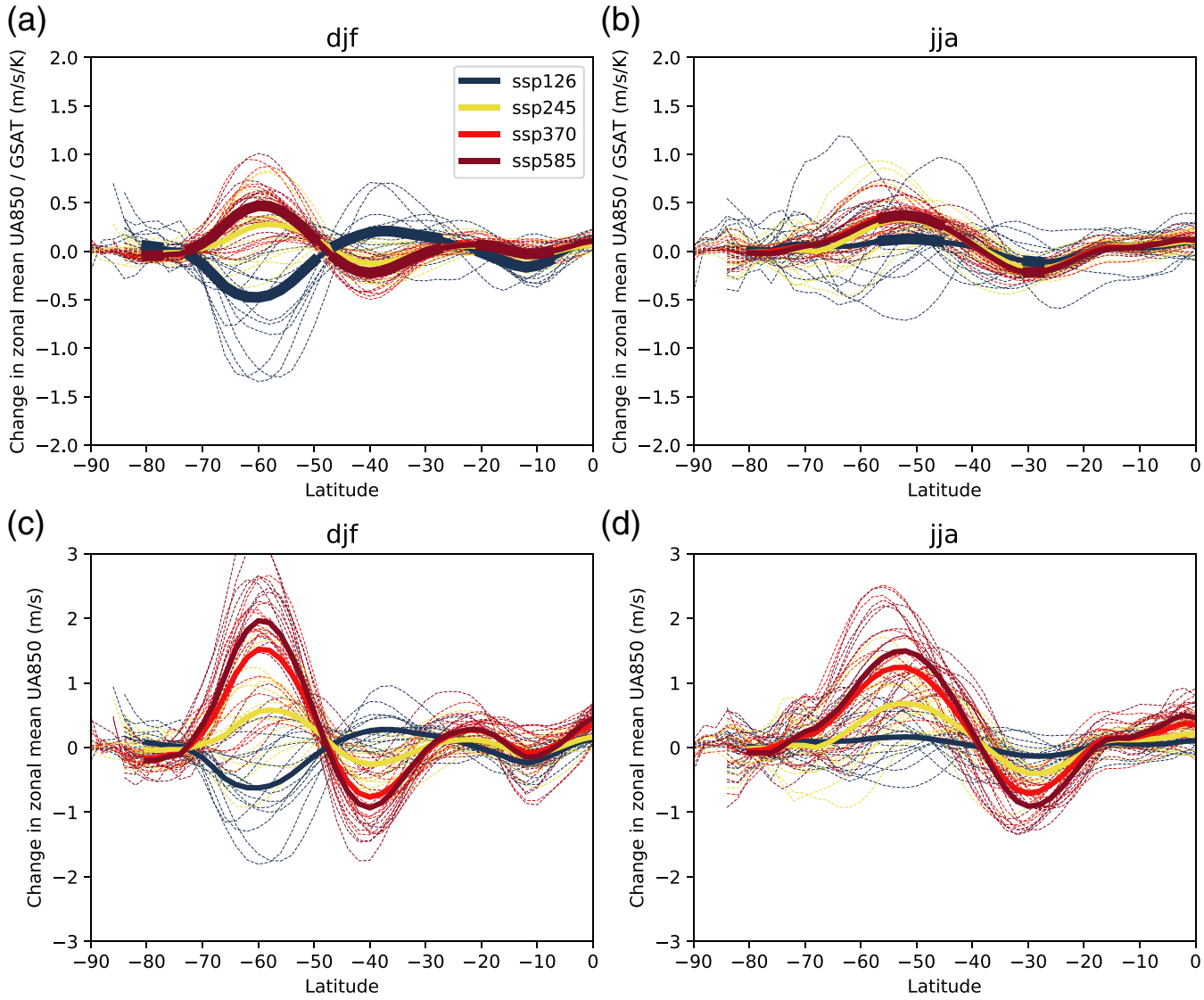

FIGURE 5 As in Figure 2, but for 850 hPa zonal (westerly) wind (i.e., the upper row (a, b) shows change relative to global mean warming in $m \cdot s^{-1} \cdot K^{-1}$)

in the latter half of the century can still play an important role and lead to differences in the DJF simulated transient climate. Figure S1 shows an ensemble mean summer (DJF) equatorward shift of the westerly jet in the SSP1-2.6 scenario, but a poleward shift in all scenarios in winter (JJA).

3.2 | Comparing early and late 21st century change

To evaluate westerly jet projections more broadly and linkages across different variables, Figures 6 and 7 show zonal mean wind changes over the first and second halves of the 21st century, along with TAS and PR changes. Following (Barnes *et al*., 2014) we define 2045 as the year for which radiative forcing scenarios (and impacts on the jet) begin to clearly diverge (Figure S1). After this point, the effects of continued stratospheric ozone recovery dominate in low forcing scenarios (as explained at the end of the previous section this increased relative importance occurs despite a weaker absolute rate of ozone recovery) whereas jet responses to increased GHGs dominate in high emissions scenarios (Figure 7). The westerly jet trends in JLI and JSI reflect the changes in zonal mean winds. As shown by Barnes *et al*. (2014) for CMIP5, there is only a weak poleward shift and strengthening in summer (DJF) during the early 21st century period with inter-scenario differences in trends then responding to divergent global mean radiative forcings in the second half of the century (Figure S1). These changes are reflected in the zonal mean zonal wind changes shown in

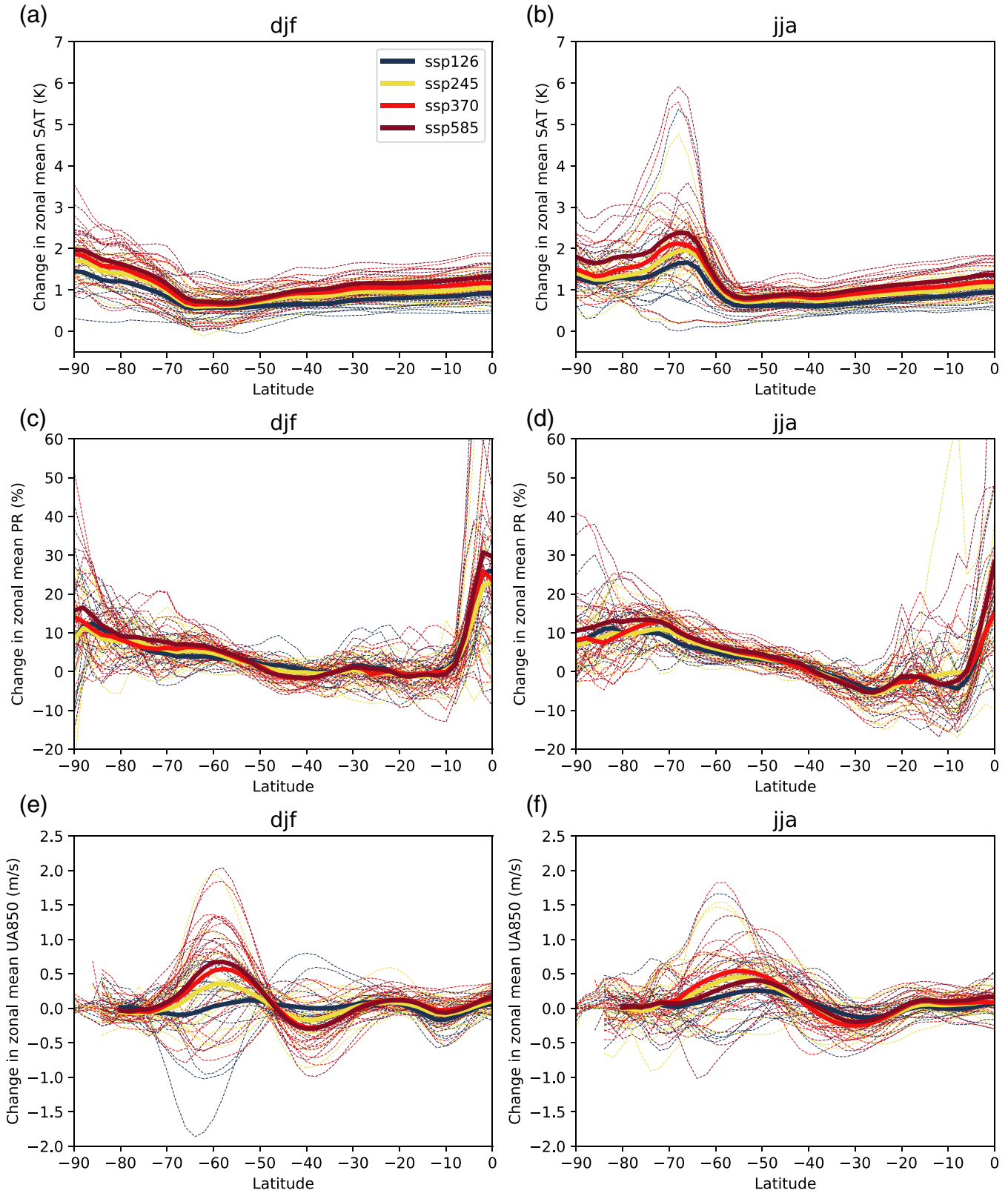

FIGURE 6 Early 21st century changes (2035–2054 minus 1995–2014) for zonal means of TAS (a, b), PR (c, d) and UA850 (e, f)

Figures 6 and 7. In particular, in Figure 7e the wide inter-scenario range in late 21st century wind projections in summer (DJF) is clear at approximately 60°S, where there is strong model consensus for large increases in SSP5-8.5 and decreases in SSP1-2.6. In SSP2-4.5 in summer there is almost no change on average across the

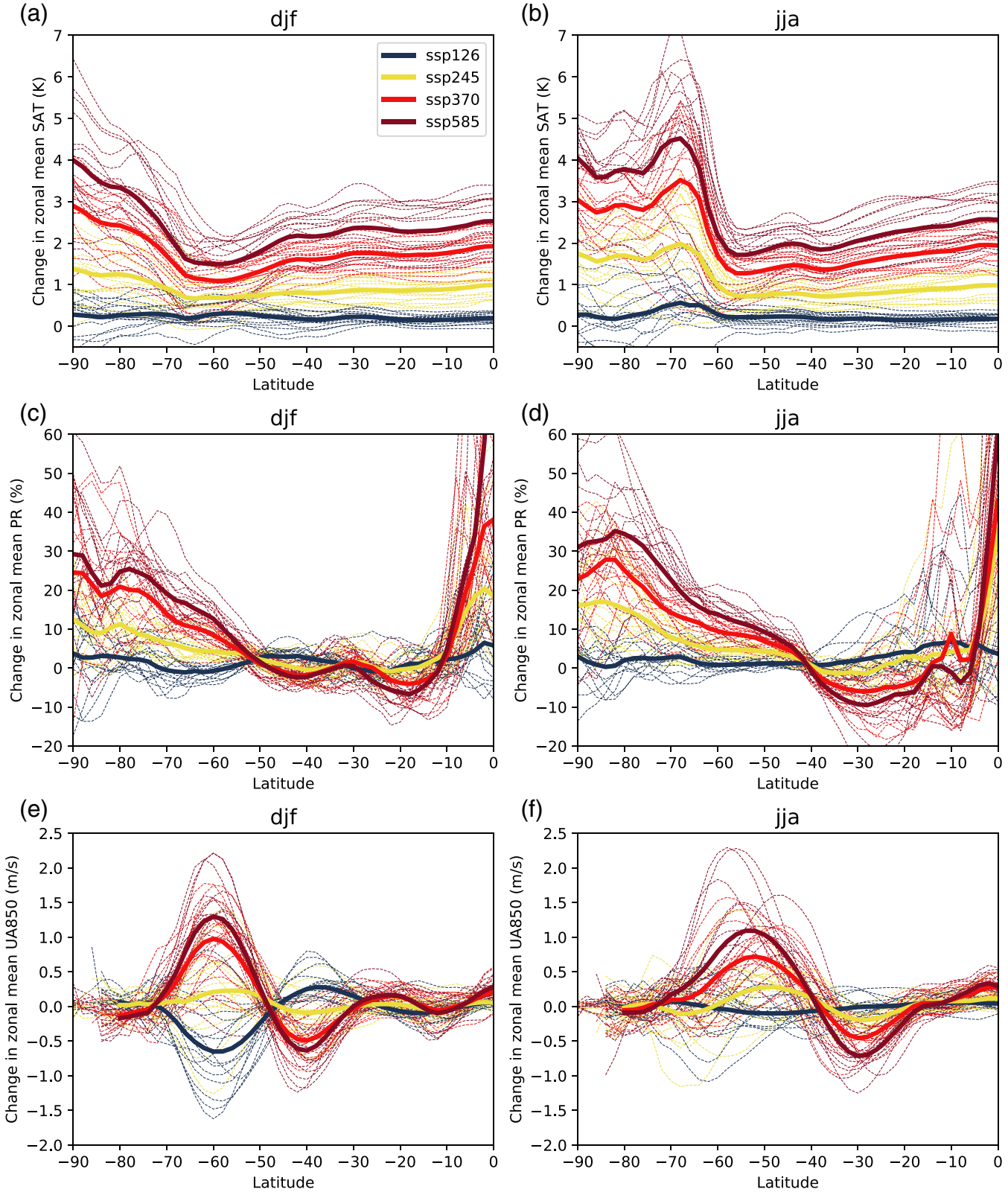

FIGURE 7 Late 21st century changes (2081–2100 minus 2035–2054) for zonal means of TAS (a, b), PR (c, d) and UA850 (e, f)

models due to cancellation between the impacts of as stratospheric ozone recovery and global radiative forcing. Interestingly, despite the weakening and equatorward shifting jet in summer in SSP1-2.6, TAS changes over the SO in this scenario still exhibit a slight warming (Figure 7a), which, although small in magnitude, is in

fact the largest in the whole Southern Hemisphere; in stark contrast with the weaker GSAT-relative SO warming that occurs in other scenarios and for the early 21st century (Figure 6a,b). It is this late 21st century divergence that brings about the inter-scenario differences in whole-century trends shown in Figure 2. This late-century divergence also illustrates linkages between the changing zonal winds and precipitation changes. In Figure 7c most models exhibit declines in precipitation rate in the SSP1-2.6 scenario between 60 and 70°S, which is on the southern flank of decreases in the zonal wind component. This minimum in precipitation rate change in not evident in winter (Figure 7d), when wind changes are much smaller in magnitude, and is also consistent with the recently-identified link between model-simulated stratospheric ozone trends and Antarctic precipitation trends (Lenaerts *et al*., 2018).

4 | CONCLUSIONS

This paper provides an initial evaluation of 21st century projected changes in temperature (SAT and SST), precipitation rate and the westerly jet over Antarctica and the SO in the four Tier-1 CMIP6 ScenarioMIP scenarios: SSP1-2.6, SSP2-4.5, SSP3-7.0 and SSP5-8.5. Ensemble mean warming across continental Antarctica is 1.3 ± 0.5, 2.5 ± 0.7, 3.7 ± 0.9 and 4.8 ± 1.2°C respectively for the four scenarios. Corresponding proportional increases in precipitation rate are 8 ± 5, 16 ± 6, 24 ± 9 and 31 ± 12%. Projected changes in the westerly jet are influenced by stratospheric ozone recovery, particularly up to mid-century. During this period, small summer jet changes are consistent with an approximate cancellation between the equatorward-shifting impact of stratospheric ozone recovery and the poleward-shift effect of increasing radiative forcing. After mid-century, the results are consistent with a dominance of global radiative forcing in the high forcing scenarios, but further ozone recovery dominating the aggressive mitigation SSP1-2.6 scenario with significant equatorward jet shifts in summer.

The results show evidence for delayed warming over the SO in the SSP1-2.6 mitigation scenario and, to a lesser degree, SSP2-4.5 stabilisation scenario, compared to projections based on SSP3-7.0 and SSP5-8.5. Consistent with this, the two lower-forcing scenarios exhibit stronger GSAT-relative warming over coastal Antarctica, but not consistently over the Antarctic interior. However, these results are preliminary and further research is required to identify the mechanisms driving regional Antarctic and SO climate responses. For example, a key question is the extent to which weakening and equatorward shifting westerlies in the SSP1-2.6 scenario may affect the strength of the above-highlighted delayed SO warming.

For precipitation projections over coastal Antarctica and the SO there is a clearer link to jet responses than for surface temperature. This is most apparent in late 21st century change following SSP1-2.6 projections, for which weaker, or in some models even negative, precipitation change occurs over coastal Antarctica as the jet shifts equatorward in summer under recovery of stratospheric ozone. This effect is however less clear over the continental interior of Antarctica, where both precipitation and temperature responses are found to follow simple relationships with global change.

A key implication of the CMIP6 projections shown in this paper is that climate projections in coastal Antarctica, in the vicinity of major ice shelves and sea ice, do not follow a simple linear relationship with global mean change (GSAT). In strong mitigation and stabilisation scenarios, there is potential for more persistent GSAT-relative Antarctic and SO warming. However, missing processes relating to freshwater fluxes from ice sheets would be important to include, ideally in a fully coupled framework, in development of the next generation of models, for example CMIP7. With regard to the results shown in this paper, inclusion of interactive ice sheets may actually lead to even larger inter-scenario differences in GSAT-relative change, as higher melt rates in high-forcing scenarios may, according to model studies, further delay warming in the SO. A further more technical implication relates to commonly used indices of polar climate change, which are generally based on spatial means over the whole of the polar cap poleward of 60°S. The results here highlight that such indices do not resolve significant differences in response characteristics between marine and terrestrial Antarctica.

ACKNOWLEDGEMENTS

Planning for this manuscript was initiated at a workshop funded by the Scientific Committee on Antarctic Research (SCAR) AntClim21 Scientific Research Programme. Bruno Ferrero is gratefully thanked for assistance in producing Figure 3. Two anonymous reviewers are thanked for their insightful and constructive comments which greatly helped to improve the manuscript. We acknowledge the World Climate Research Programme, which, through its Working Group on Coupled Modelling, coordinated and promoted CMIP6. We thank the climate modelling groups for producing and making available their model output, the Earth System Grid Federation (ESGF) for archiving the data and providing access, and the multiple funding agencies who support CMIP6 and ESGF. The Centre for Environmental Data Analysis (CEDA) and JASMIN provided the platform for much of the data analysis conducted. T. J. B. and K. A. N. were supported by the UK Natural Environment Research Council (NERC) through the British Antarctic

Survey research programme Polar Science for Planet Earth. K. A. N. and T. J. B. were additionally supported by NERC projects NE/L013770/1 and NE/N01829X/1 respectively. F. A. H. was supported by the SNSF grant numbers P2EZP2_175162 and P400P2_186681, as well as NSF's SOCCOM Project under NSF Award No. PLR-1425989. Support for M. T. and I. W. provided by grants CNPq–MCT–INCT–594 CRIOSFERA 573720/2008–8 and Coordenação de Aperfeiçoamento de Pessoal de Nível Superior–Brasil (CAPES)–Finance Code 001. L. R. was supported by National Science Foundation grant PLR-1643431 and National Oceanic and Atmospheric Administration grant NA18OAR4310274. T.R. was funded by the Alfred Wegener Institute, Helmholtz Centre for Polar and Marine Research, Germany.

SUPPORTING INFORMATION

This manuscript includes supporting information Figure S1, which shows time series of JLI and JSI for multiple models and scenarios through the 21st century.

ORCID

Thomas J. Bracegirdle https://orcid.org/0000-0002-8868-4739
Gerhard Krinner https://orcid.org/0000-0002-2959-5920
F. Alexander Haumann https://orcid.org/0000-0002-8218-977X
Lettie A. Roach https://orcid.org/0000-0003-4189-3928

REFERENCES

Armour, K.C., Marshall, J., Scott, J.R., Donohoe, A. and Newsom, E.R. (2016) Southern Ocean warming delayed by circumpolar upwelling and equatorward transport. *Nature Geoscience*, 9(7), 549–554. https://doi.org/10.1038/ngeo2731.

Asay-Davis, X.S., Cornford, S.L., Durand, G., Galton-Fenzi, B.K., Gladstone, R.M., Gudmundsson, G.H., Hattermann, T., Holland, D.M., Holland, D., Holland, P.R., Martin, D.F., Mathiot, P., Pattyn, F. and Seroussi, H. (2016) Experimental design for three interrelated marine ice sheet and ocean model intercomparison projects: MISMIP v. 3 (MISMIP+), ISOMIP v. 2 (ISOMIP+) and MISOMIP v. 1 (MISOMIP1). *Geoscientific Model Development*, 9(7), 2471–2497. https://doi.org/10.5194/gmd-9-2471-2016.

Barnes, E.A., Barnes, N.W. and Polvani, L.M. (2014) Delayed southern hemisphere climate change induced by stratospheric ozone recovery, as projected by the CMIP5 models. *Journal of Climate*, 27(2), 852–867. https://doi.org/10.1175/jcli-d-13-00246.1.

Bracegirdle, T.J., Stephenson, D.B., Turner, J. and Phillips, T. (2015) The importance of sea ice area biases in 21st century multimodel projections of Antarctic temperature and precipitation. *Geophysical Research Letters*, 42(24), 10832–10839. https://doi.org/10.1002/2015gl067055.

Bromwich, D.H., Chen, B. and Hines, K.M. (1998) Global atmospheric impacts induced by year-round open water adjacent to Antarctica. *Journal of Geophysical Research*, 103, 11173–11189.

Bronselaer, B., Winton, M., Griffies, S.M., Hurlin, W.J., Rodgers, K. B., Sergienko, O.V., Stouffer, R.J. and Russell, J.L. (2018) Change in future climate due to Antarctic meltwater. *Nature*, 564(7734), 53–58. https://doi.org/10.1038/s41586-018-0712-z.

Bushinsky, S.M., Landschutzer, P., Rodenbeck, C., Gray, A.R., Baker, D., Mazloff, M.R., Resplandy, L., Johnson, K.S. and Sarmiento, J.L. (2019) Reassessing Southern Ocean Air-Sea CO2 flux estimates with the addition of biogeochemical float observations. *Global Biogeochemical Cycles*, 33(11), 1370–1388. https://doi.org/10.1029/2019gb006176.

De Rydt, J. and Gudmundsson, G.H. (2016) Coupled ice shelf-ocean modeling and complex grounding line retreat from a seabed ridge. *Journal of Geophysical Research-Earth Surface*, 121(5), 865–880. https://doi.org/10.1002/2015jf003791.

DeConto, R.M. and Pollard, D. (2016) Contribution of Antarctica to past and future sea-level rise. *Nature*, 531(7596), 591–597. https://doi.org/10.1038/nature17145.

Dhomse, S.S., Kinnison, D., Chipperfield, M.P., Salawitch, R.J., Cionni, I., Hegglin, M.I., Abraham, N.L., Akiyoshi, H., Archibald, A.T., Bednarz, E.M., Bekki, S., Braesicke, P., Butchart, N., Dameris, M., Deushi, M., Frith, S., Hardiman, S. C., Hassler, B., Horowitz, L.W., Hu, R.M., Jöckel, P., Josse, B., Kirner, O., Kremser, S., Langematz, U., Lewis, J., Marchand, M., Lin, M., Mancini, E., Marécal, V., Michou, M., Morgenstern, O., O'Connor, F.M., Oman, L., Pitari, G., Plummer, D.A., Pyle, J.A., Revell, L.E., Rozanov, E., Schofield, R., Stenke, A., Stone, K., Sudo, K., Tilmes, S., Visioni, D., Yamashita, Y. and Zeng, G. (2018) Estimates of ozone return dates from chemistry-climate model initiative simulations. *Atmospheric Chemistry and Physics*, 18(11), 8409–8438. https://doi.org/10.5194/acp-18-8409-2018.

England, M., Polvani, L. and Sun, L.T. (2018) Contrasting the Antarctic and Arctic atmospheric responses to projected sea ice loss in the late twenty-first century. *Journal of Climate*, 31(16), 6353–6370. https://doi.org/10.1175/jcli-d-17-0666.1.

Eyring, V., Waugh, D.W., Bodeker, G.E., Cordero, E., Akiyoshi, H., Austin, J., Beagley, S.R., Boville, B.A., Braesicke, P., Brühl, C., Butchart, N., Chipperfield, M.P., Dameris, M., Deckert, R., Deushi, M., Frith, S.M., Garcia, R.R., Gettelman, A., Giorgetta, M.A., Kinnison, D.E., Mancini, E., Manzini, E., Marsh, D.R., Matthes, S., Nagashima, T., Newman, P.A., Nielsen, J.E., Pawson, S., Pitari, G., Plummer, D.A., Rozanov, E., Schraner, M., Scinocca, J.F., Semeniuk, K., Shepherd, T.G., Shibata, K., Steil, B., Stolarski, R.S., Tian, W. and Yoshiki, M. (2007) Multimodel projections of stratospheric ozone in the 21st century. *Journal of Geophysical Research-Atmospheres*, 112, D16303. https://doi.org/10.1029/2006jd008332.

Eyring, V., Bony, S., Meehl, G.A., Senior, C.A., Stevens, B., Stouffer, R.J. and Taylor, K.E. (2016) Overview of the coupled model Intercomparison project phase 6 (CMIP6) experimental design and organization. *Geoscientific Model Development*, 9(5), 1937–1958. https://doi.org/10.5194/gmd-9-1937-2016.

Favier, L., Jourdain, N.C., Jenkins, A., Merino, N., Durand, G., Gagliardini, O., Gillet-Chaulet, F. and Mathiot, P. (2019) Assessment of sub-shelf melting parameterisations using the ocean-ice-sheet coupled model NEMO(v3.6)-Elmer/Ice(v8.3). *Geoscientific Model Development*, 12(6), 2255–2283. https://doi.org/10.5194/gmd-12-2255-2019.

Frölicher, T.L., Sarmiento, J.L., Paynter, D.J., Dunne, J.P., Krasting, J.P. and Winton, M. (2015) Dominance of the Southern Ocean in anthropogenic carbon and heat uptake in CMIP5 models. *Journal of Climate*, 28(2), 862–886. https://doi.org/10.1175/jcli-d-14-00117.1.

Goddard, P.B., Dufour, C.O., Yin, J.J., Griffies, S.M. and Winton, M. (2017) CO2-Induced Ocean warming of the Antarctic continental shelf in an eddying global climate model. *Journal of Geophysical Research-Oceans*, 122(10), 8079–8101. https://doi.org/10.1002/2017jc012849.

Golledge, N.R., Thomas, Z.A., Levy, R.H., Gasson, E.G.W., Naish, T.R., McKay, R.M., Kowalewski, D.E. and Fogwill, C.J. (2017) Antarctic climate and ice-sheet configuration during the early Pliocene interglacial at 4.23 Ma. *Climate of the Past*, 13(7), 959–975. https://doi.org/10.5194/cp-13-959-2017.

Golledge, N.R., Keller, E.D., Gomez, N., Naughten, K.A., Bernales, J., Trusel, L.D. and Edwards, T.L. (2019) Global environmental consequences of twenty-first-century ice-sheet melt. *Nature*, 566(7742), 65–72. https://doi.org/10.1038/s41586-019-0889-9.

Gruber, N., Clement, D., Carter, B.R., Feely, R.A., van Heuven, S., Hoppema, M., Ishii, M., Key, R.M., Kozyr, A., Lauvset, S.K., Lo Monaco, C., Mathis, J.T., Murata, A., Olsen, A., Perez, F.F., Sabine, C.L., Tanhua, T. and Wanninkhof, R. (2019) The oceanic sink for anthropogenic CO2 from 1994 to 2007. *Science*, 363(6432), 1193–1199. https://doi.org/10.1126/science.aau5153.

Hansen, J., Sato, M., Hearty, P., Ruedy, R., Kelley, M., Masson-Delmotte, V., Russell, G., Tselioudis, G., Cao, J., Rignot, E., Velicogna, I., Tormey, B., Donovan, B., Kandiano, E., von Schuckmann, K., Kharecha, P., Legrande, A.N., Bauer, M. and Lo, K.W. (2016) Ice melt, sea level rise and superstorms: evidence from paleoclimate data, climate modeling, and modern observations that 2 A degrees C global warming could be dangerous. *Atmospheric Chemistry and Physics*, 16(6), 3761–3812. https://doi.org/10.5194/acp-16-3761-2016.

Hellmer, H.H., Kauker, F., Timmermann, R. and Hattermann, T. (2017) The fate of the southern Weddell Sea continental shelf in a warming climate. *Journal of Climate*, 30(12), 4337–4350. https://doi.org/10.1175/jcli-d-16-0420.1.

Hwang, Y.T., Xie, S.P., Deser, C. and Kang, S.M. (2017) Connecting tropical climate change with Southern Ocean heat uptake. *Geophysical Research Letters*, 44(18), 9449–9457. https://doi.org/10.1002/2017gl074972.

Jenouvrier, S., Holland, M., Stroeve, J., Serreze, M., Barbraud, C., Weimerskirch, H. and Caswell, H. (2014) Projected continent-wide declines of the emperor penguin under climate change. *Nature Climate Change*, 4(8), 715–718. https://doi.org/10.1038/nclimate2280.

Karpechko, A.Y., Gillett, N.P., Gray, L.J. and Dall'Amico, M. (2010) Influence of ozone recovery and greenhouse gas increases on southern hemisphere circulation. *Journal of Geophysical Research-Atmospheres*, 115, D22117. https://doi.org/10.1029/2010jd014423.

Lee, J.R., Raymond, B., Bracegirdle, T.J., Chades, I., Fuller, R.A., Shaw, J.D. and Terauds, A. (2017) Climate change drives expansion of Antarctic ice-free habitat. *Nature*, 547(7661), 49–54. https://doi.org/10.1038/nature22996.

Lenaerts, J.T.M., Fyke, J. and Medley, B. (2018) The signature of ozone depletion in recent Antarctic precipitation change: a study with the community earth system model. *Geophysical Research Letters*, 45(23), 12931–12939. https://doi.org/10.1029/2018gl078608.

Li, C., Notz, D., Tietsche, S. and Marotzke, J. (2013) The transient versus the equilibrium response of sea ice to global warming. *Journal of Climate*, 26(15), 5624–5636. https://doi.org/10.1175/jcli-d-12-00492.1.

Manabe, S., Stouffer, R.J., Spelman, M.J. and Bryan, K. (1991) Transient responses of a coupled ocean atmosphere model to gradual changes of atmospheric CO2. 1. Annual mean response. *Journal of Climate*, 4(8), 785–818. https://doi.org/10.1175/1520-0442(1991)004<0785:troaco>2.0.co;2.

Meinshausen, M., Smith, S.J., Calvin, K., Daniel, J.S., Kainuma, M. L.T., Lamarque, J.F., Matsumoto, K., Montzka, S.A., Raper, S. C.B., Riahi, K., Thomson, A., Velders, G.J.M. and van Vuuren, D.P.P. (2011) The RCP greenhouse gas concentrations and their extensions from 1765 to 2300. *Climatic Change*, 109 (1–2), 213–241. https://doi.org/10.1007/s10584-011-0156-z.

O'Neill, B.C., Tebaldi, C., van Vuuren, D.P., Eyring, V., Friedlingstein, P., Hurtt, G., Knutti, R., Kriegler, E., Lamarque, J.-F., Lowe, J., Meehl, G.A., Moss, R., Riahi, K. and Sanderson, B.M. (2016) The scenario model Intercomparison project (ScenarioMIP) for CMIP6. *Geoscientific Model Development*, 9(9), 3461–3482. https://doi.org/10.5194/gmd-9-3461-2016.

Perlwitz, J., Pawson, S., Fogt, R.L., Nielsen, J.E. and Neff, W.D. (2008) Impact of stratospheric ozone hole recovery on Antarctic climate. *Geophysical Research Letters*, 35(8), L08714. https://doi.org/10.1029/2008gl033317.

Rintoul, S.R., Chown, S.L., DeConto, R.M., England, M.H., Fricker, H.A., Masson-Delmotte, V., Naish, T.R., Siegert, M.J. and Xavier, J.C. (2018) Choosing the future of Antarctica. *Nature*, 558(7709), 233–241. https://doi.org/10.1038/s41586-018-0173-4.

Rohling, E.J., Hibbert, F.D., Grant, K.M., Galaasen, E.V., Irvali, N., Kleiven, H.F., Marino, G., Ninnemann, U., Roberts, A.P., Rosenthal, Y., Schulz, H., Williams, F.H. and Yu, J. (2019) Asynchronous Antarctic and Greenland ice-volume contributions to the last interglacial sea-level highstand. *Nature Communications*, 10, 5040. https://doi.org/10.1038/s41467-019-12874-3.

Salzmann, M. (2017) The polar amplification asymmetry: role of Antarctic surface height. *Earth System Dynamics*, 8(2), 323–336. https://doi.org/10.5194/esd-8-323-2017.

Smith, K.L., Polvani, L.M. and Marsh, D.R. (2012) Mitigation of 21st century Antarctic Sea ice loss by stratospheric ozone recovery. *Geophysical Research Letters*, 39, L20701. https://doi.org/10.1029/2012gl053325.

Son, S.W., Polvani, L.M., Waugh, D.W., Akiyoshi, H., Garcia, R., Kinnison, D., Pawson, S., Rozanov, E., Shepherd, T.G. and Shibata, K. (2008) The impact of stratospheric ozone recovery on the southern hemisphere westerly jet. *Science*, 320(5882), 1486–1489. https://doi.org/10.1126/science.1155939.

Stewart, A.L. and Thompson, A.F. (2015) Eddy-mediated transport of warm circumpolar deep water across the Antarctic shelf break. *Geophysical Research Letters*, 42(2), 432–440. https://doi.org/10.1002/2014gl062281.

Taylor, K.E., Stouffer, R.J. and Meehl, G.A. (2012) An overview of CMIP5 and the experiment design. *Bulletin of the American Meteorological Society*, 93, 485–498. https://doi.org/10.1175/bams-d-11-00094.1.

Thompson, D.W.J. and Solomon, S. (2002) Interpretation of recent southern hemisphere climate change. *Science*, 296, 895–899. https://doi.org/10.1126/science.1069270.

Thompson, A.F., Stewart, A.L., Spence, P. and Heywood, K.J. (2018) The Antarctic slope current in a changing climate. *Reviews of Geophysics*, 56(4), 741–770. https://doi.org/10.1029/2018rg000624.

Turner, J., Barrand, N.E., Bracegirdle, T.J., Convey, P., Hodgson, D.A., Jarvis, M., Jenkins, A., Marshall, G., Meredith, M.P., Roscoe, H., Shanklin, J., French, J., Goosse, H., Guglielmin, M., Gutt, J., Jacobs, S., Kennicutt, M.C., II, Masson-Delmotte, V., Mayewski, P., Navarro, F., Robinson, S., Scambos, T., Sparrow, M., Summerhayes, C., Speer, K. and Klepikov, A. (2014) Antarctic climate change and the environment: an update. *Polar Record*, 50(3), 237–259. https://doi.org/10.1017/s0032247413000296.

Wilcox, L.J., Charlton-Perez, A.J. and Gray, L.J. (2012) Trends in austral jet position in ensembles of high- and low-top CMIP5 models. *Journal of Geophysical Research—Atmospheres*, 117, D13115. https://doi.org/10.1029/2012JD017597.

SUPPORTING INFORMATION

Additional supporting information may be found online in the Supporting Information section at the end of this article.

How to cite this article: Bracegirdle TJ, Krinner G, Tonelli M, *et al.* Twenty first century changes in Antarctic and Southern Ocean surface climate in CMIP6. *Atmos Sci Lett*. 2020;21:e984. https://doi.org/10.1002/asl.984